Organic & Biomolecular Chemistry

ROYAL SOCIETY OF CHEMISTRY

PAPER

View Article Online
View Journal | View Issue

Cite this: *Org. Biomol. Chem.*, 2021, **19**, 2008

Identification of organophosphorus simulants for the development of next-generation detection technologies†

Rebecca J. Ellaby,[a] Ewan R. Clark,*[a] Nyasha Allen,[b] Faith R. Taylor,[a] Kendrick K. L. Ng,[a] Milan Dimitrovski,[a] Dominique F. Chu,[c] Daniel P. Mulvihill[b] and Jennifer R. Hiscock *[a]

Received 17th December 2020,
Accepted 9th February 2021

DOI: 10.1039/d0ob02523b

rsc.li/obc

Organophosphorus (OP) chemical warfare agents (CWAs) represent an ongoing threat but the understandable widespread prohibition of their use places limitations on the development of technologies to counter the effects of any OP CWA release. Herein, we describe new, accessible methods for the identification of appropriate molecular simulants to mimic the hydrogen bond accepting capacity of the P═O moiety, common to every member of this class of CWAs. Using the predictive methodologies developed herein, we have identified OP CWA hydrogen bond acceptor simulants for soman and sarin. It is hoped that the effective use of these physical property specific simulants will aid future countermeasure developments.

Introduction

Organophosphorus (OP) compounds have been used on a global scale as pesticides and chemical warfare agents (CWAs) for almost a century.[1] The uncontrolled release of these highly toxic compounds presents a continuing global risk as evidenced by recent small-scale events within Germany (2020),[2] the UK (2018)[3] and Malaysia (2017),[4] combined with larger-scale events in Syria (2013)[5] and Japan (1995).[6] The development of novel detection technologies is therefore of high global importance.

Recently, supramolecular systems have been effectively targeted to fulfil this need.[7] This has included the development of fluorescent[8] and luminescent sensors,[9–11] and a body of work from Gale and co-workers in which hydrogen bond donating compounds have been shown to: selectively form OP CWA hydrogen bonded complexes;[12,13] act as OP CWA hydrolysis organocatalysts;[14] produce supramolecular organogels that act both as OP CWA sensory and decontamination materials.[15–17] Additionally, Cragg and co-workers have developed a crown-(thio)urea based receptor capable of sensing the presence of sarin and soman hydrolysis breakdown products.[18] Here the resultant fluoride ion binds to the thio(urea) moiety, while the phosphate group coordinates to the crown ether, resulting in a colourless to orange colorimetric change. Finally, a body of work by Ward and co-workers has shown that self-assembled cages can bind CWA simulants inducing a fluorescence response,[19] and act as catalysts for the hydrolysis of phospho-ester species.[20]

OP simulants are typically the only available option for developing novel approaches to combat OP CWA release due to the highly toxic nature of, and legal restrictions placed upon, the live agents themselves. However, no single simulant can simultaneously mimic all the chemical properties of an OP CWA without also inheriting undesirable molecular traits. It is therefore vital to consider the appropriate properties of any simulant chosen to aid in the development of novel OP CWA detection, decontamination, or remediation methodologies.[21–24] Recently, work undertaken by Snurr and Mendonca, has shown that density functional theory (DFT) can be used to study the mechanism of OP hydrolysis, which has resulted in the development of a quantitative structure activity relationship (QSAR) model that enables the identification of appropriate OP CWA simulants for decontamination purposes.[25]

However, when considering supramolecular technologies, the moiety target is often selective coordination of the polar P═O functionality. This chemical group, common to all OP CWAs, plays a significant role in both molecular surface coordination properties and reactivity. Herein, we extend our

[a]*School of Physical Sciences, University of Kent, Park Wood Road, Canterbury, Kent, CT2 7NH, UK. E-mail: J.R.Hiscock@Kent.ac.uk, E.R.Clark@Kent.ac.uk; Tel: +44(0) 1227 816467, +44(0) 1227 816152*

[b]*School of Biosciences, University of Kent, Park Wood Road, Canterbury, Kent, CT2 7NH, UK*

[c]*School of Computing, University of Kent, Darwin Road, Canterbury, Kent, CT2 7NZ, UK*

†Electronic supplementary information (ESI) available: Experimental details, mass spectrometry, NMR, crystallography‡ and computational modelling data. CCDC 1855728. For ESI and crystallographic data in CIF or other electronic format see DOI: 10.1039/d0ob02523b

prior work, which showed that simple, low level computational modelling may be used to predict hydrogen bond mediated aggregation events[26,27] and antimicrobial activity,[28] to identify appropriate OP CWA simulants for the development of supramolecular detection technologies, complementing the recent advances made in this area for hydrolysis siumulants.[25]

Here, we hypothesised that neutral hydrogen bond donating receptors **1–4** (Fig. 1) would form hydrogen bonded complexes with potential OP CWA simulants (**5–26**) and, due to the structural simplicity of **1–4**, the strength of the complex formed would depend on the properties associated with the principal hydrogen bond acceptor (HBA) group. The association constants (K_{ass}) relating to these hydrogen bonded complexation processes should therefore provide information relating to the simulants' principal HBA site, which corresponds to the moiety mimicking the P═O group of a specific OP CWA. These experimental data are then correlated with parameters derived from accessible computational modelling methods, to enable the identification of an appropriate simulant. Compounds **11–15** are commercially available species commonly used to simulate OP CWAs. The structures of simulants **5–10** and **16–26** were designed to fulfil the following criteria: charge neutrality; not readily ionised under experimental conditions; containing a single electrophilic site (S or P); and containing a single HBA centre (either a P═O (**5–15**), or O═S═O (**16–26**)).

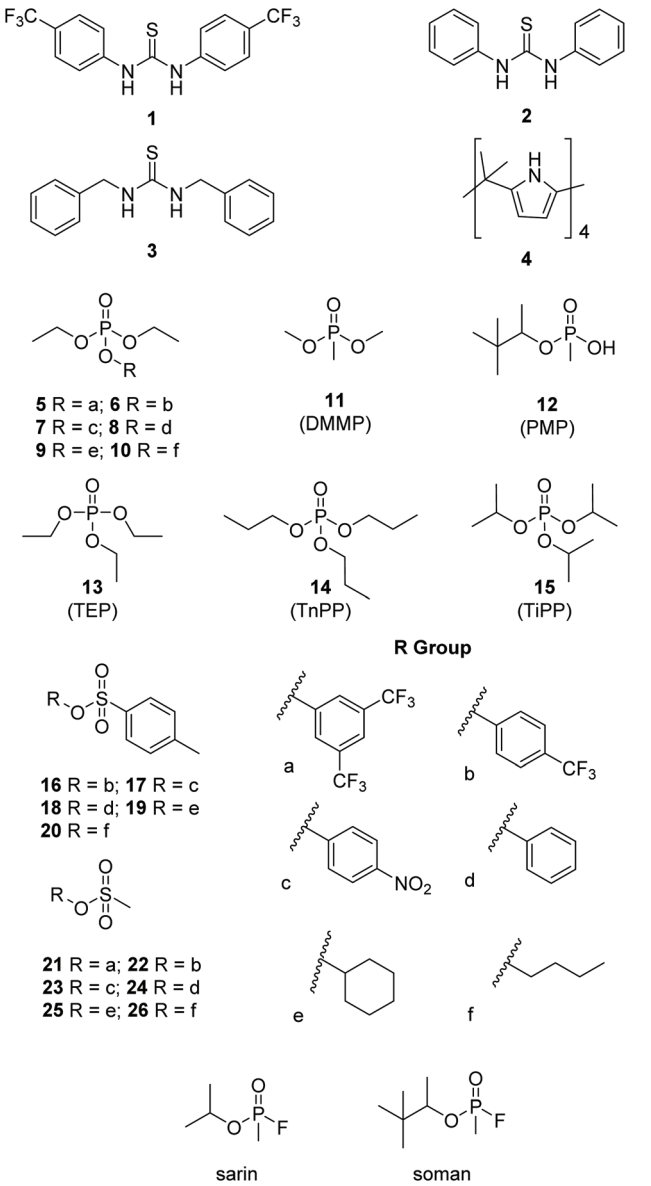

Fig. 1 Chemical structure of **1–26**, sarin and soman.

Synthesis

The syntheses of **1–4**, **7–9**, **17–21**, and **23–26** have previously been reported.[29–40] Compounds **5**, **6** and **10** were obtained as colourless oils in 65%, 90%, and 85% yields respectively, from the reaction of diethyl chlorophosphate with the respective alcohol in chloroform. Compound **16** was obtained as a white solid in a 59% yield from the reaction of 4-(trifluoromethyl) phenol with *p*-toluene sulfonylchloride in chloroform. Compound **22** was obtained as a pale-yellow solid in a 91% yield from the reaction of 4-(trifluoromethyl)phenol with methylsulfonyl chloride in chloroform.

Results and discussion

Association constant determination

Experimental association constants for receptor : simulant complexes were determined in CD_3CN using ^1H NMR titration techniques, following the downfield change in chemical shift of the thiourea/pyrrole NH resonances upon increasing concentration of the simulant with respect to the appropriate receptor (**1–4**). In all cases the experimental data were fitted to 1 : 1, 2 : 1, and 1 : 2 host : guest binding isotherms using Bindfit v0.5.[41] The errors produced from fitting these data were compared and found to support the formation of 1 : 1 receptor : simulant complexes. Job plot experiments were also performed but did not give conclusive results.[42]

A series of initial association studies were conducted to identify a lead receptor; the results are summarised in Table 1. Here, only the most acidic receptor (**1**) was found to produce association constants that span the ≥two orders of magnitude necessary to validate our hypothesis. Therefore, further data analysis utilises results obtained with **1** only. These initial results were then expanded to include all simulants (**5–26**); this final data set is given in Table 2.

A single crystal X-ray structure,‡ obtained for a 1 : 1 complex of **1** and DMSO (Fig. 2), shows the formation of one hydrogen

‡A suitable crystal of **1** with DMSO was selected and mounted on a Rigaku Oxford Diffraction Supernova diffractometer. Data were collected using Cu Kα radiation at 100 K. Structures were solved with ShelXT[55] structure solution programmes *via* direct methods and refined with ShelXL[56] on least squares minimisation. Olex2[57] was used as an interface to all ShelX programmes.

Table 1 K_{ass} (M^{-1}) calculated for **1–4** with potential simulants **5**, **6**, **8**, **10**, **16**, **18** and **20** in a CD_3CN solution at 298 K, obtained through the fitting of ^1H NMR titration data to a 1 : 1 host : guest binding isotherm using Bindfit v0.5[41]

No.	1	2	3	4
5	36 (±6%)	<10	19 (±11%)	<10
6	17 (±1%)	20 (±5%)	27 (±9%)	[b]
8	<10	23 (±4%)	<10	[b]
10	<10	32 (±7%)	<10	[a]
16	25 (±7%)	[a]	[a]	[a]
18	<10	19 (±6%)	[a]	[a]
20	106 (±8%)	[a]	[a]	[a]

[a] Data could not be fitted to either a 1 : 1, 2 : 1 or 1 : 2 binding isotherm. [b] Peak overlap prevented binding constant determination.

Table 2 K_{ass} (M^{-1}) calculated for **1** with **5–26** in a CD_3CN solution at 298 K, obtained through the fitting of ^1H NMR titration data to a 1 : 1 host : guest binding isotherm using Bindfit v0.5[41]

Simulant	K_{ass}	Simulant	K_{ass}
5	36 (±6%)	**16**	25 (±7%)
6	17 (±1%)	**17**	<10
7	<10	**18**	<10
8	<10	**19**	48 (±11%)
9	<10	**20**	106 (±8%)
10	<10	**21**	41 (±8%)
11	11 (±1%)	**22**	64 (±5%)
12	52 (±6%)	**23**	46 (±9%)
13	<10	**24**	76 (±6%)
14	<10	**25**	<10
15	12 (±2%)	**26**	<10

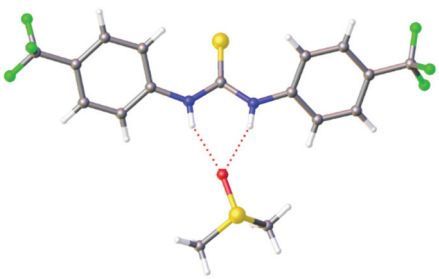

Fig. 2 Single crystal X-ray structure showing **1** binding a single DMSO solvent molecule through the formation of two hydrogen bonds. Disorder associated with the DMSO molecule and CF_3 moieties have been omitted for clarity. Grey = carbon; white = hydrogen; green = fluorine; blue = nitrogen; yellow = sulphur. Red dashed line indicates hydrogen bonding.

bond from each of the thiourea NH groups to the S=O HBA group of the DMSO solvent molecule. It is therefore reasonable to hypothesise that the analogous hydrogen bonded complexes may be formed between **1** and simulants **5–15**, which contain a single oxygen atom acting as the principal HBA (Fig. 3c). However, when considering simulants **16–26**, the possibility exists that, because of the two HBA oxygen atoms within

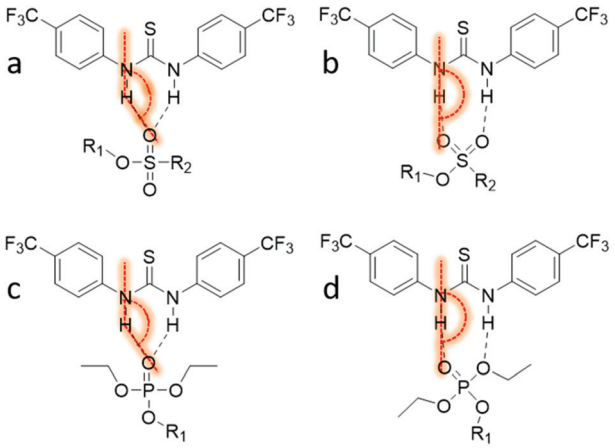

Fig. 3 Possible binding modes for the formation of 1 : 1 complexes of **1** with (a) **16–26**, (b) **16–26**, (c) **5–15** and (d) **5–15**. Hydrogen bonding angles are shown in red.

the sulfonate group, the formation of hydrogen bonds may be permitted to one (Fig. 3a, O1′) or both of these atoms (Fig. 3b, O2′).

In-silico modelling

As it is feasible that **16–26** could adopt one of two 1 : 1 binding modes with **1** (Fig. 3b and c), the potential for one of these binding modes prevailing within the solution state was further explored computationally (M06-2X/6-311 g(d,p)), (PCM = acetonitrile, Gaussian16).[43–45]

The geometries of **6**, **9**, **10**, **11**, **16–20**, **25**, **26**, sarin and soman with receptor **1**, were optimised individually and as interacting pairs in both O1′ and O2′ configurations.† These calculations confirmed the viability of both O1′ and O2′ binding modes for the sulfonyl species. However, as expected no stable O2′ binding modes were found for the phosphonyl species (Fig. 3d). The energies of binding are significant (−41.2 to −84.6 kJ mol^{-1}) for both sulfonyl and phosphonyl species, with no clear preference for O1′ over O2′ found for the sulfonyls, although significant substituent dependence was observed. This is attributed to the variable changes in steric profile on moving the simulant between O1′ and O2′ bonding and the resultant effect on secondary interactions.

Having confirmed the binding modes, we then sought to develop an accessible predictive model for association strength. DFT (M06-2X/6-311 g(d,p)) is a good computational model for systems such as these as it accounts for non-covalent interactions but is computationally expensive.[46] We have previously shown that low-level calculations can supply useful guest-only parameters for predicting trends in association constant without significant computational overhead. Reducing the size of the calculations requires far less computational time; additionally, Spartan '16 runs on a conventional desktop making this approach accessible to a wider chemical audience. The range of parameters output by default for

PM6 calculations is sparse, and so to expand the scope of searchable parameter space, DFT (B3LYP/6-3G1*) calculations were also performed using Spartan '16.[47–49] The analogous parameters obtained were consistent with those values produced from PM6 and M06-2X/6-311 g(d,p) calculations.† In total, a list of 19 computationally derived parameters (*P*), summarised in Table 3, were produced for each potential simulant/OP CWA alone or when in a 1 : 1 complex with **1**. This list of parameters are easily accessible, unfiltered by assumption of their relevance to avoid prejudicing the parametric search. These parameters were then used alongside the experimentally derived association constant data (Table 2) to produce initial predictive association constant models.

Single parameter predictive models

Initial comparison identified correlations between the experimentally derived association constants and host : guest hydrogen bond angle (obtained from B3LYP-6-31G* calculations), Fig. 4. For ease of interpretation, the hydrogen bond angles involved in complex formation are represented as the sum of the difference from the optimal 180° hydrogen bonding angle for those hydrogen bonds formed during the potential simulant : receptor complexation processes,[50,51] such as those exemplified in Fig. 3. Here, we identify three trends, one for the phosphoryl species and two for the sulfonyl species. The two trends identified for the sulfonyl species correspond to the two different classes of sulfonate molecules present within the library of simulants studied, those substituted with a toluene group (**16–20**) and those substituted with a methyl group (**21–26**). As the limitation of the experimental association constant determination methodology is ≈10 M^{-1}, we suggest that any values incorporating ≤10 M^{-1} may be considered inappropriate when included into a model such as this and should be treated with caution. We hypothesise that for a complex formed utilising a single HBA atom, increasing hydrogen bonding strength will result in an overall decrease in hydrogen bonding angle away from 180°, as the host and guest move closer together, resulting in a positive correlation as observed for the phosphoryl species (blue and black trends, Fig. 4). However, for complexes formed using two HBA oxygen atoms, the hydrogen bonding angles will move towards 180°, resulting in a negative correlation as observed for both sulfonate species (blue and black trends, Fig. 4). The two different trends observed for the methyl and toluene substituted sulphonyl groups we believe are due to additional R-group specific interactions.

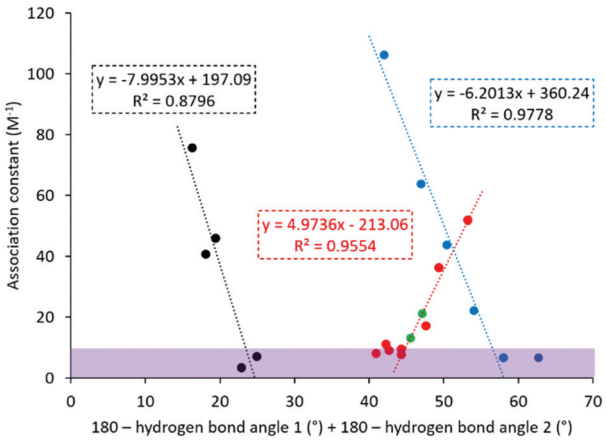

Fig. 4 One parameter association constant (K_{ass}) prediction. Red = phosphoryl species; blue = toluene substituted sulfonyl species; black = methyl substituted sulfonyl species; green = predicted OP CWAs; purple shaded section = $K_{ass} \leq 10$ M^{-1}.

The OP CWA association constants were then predicted for sarin and soman (Fig. 4, green), using the trend shown for the phosphoryl species (Fig. 4, red), resulting in predicted association constant values of 22 M^{-1} and 13 M^{-1} for sarin and soman respectively. Using the three trends shown in Fig. 4, compounds **6** and **16** were identified as the most appropriate simulants for sarin, while **10** and **11** were identified as the most appropriate simulants for soman.

Exhaustive parameter search

The energetics of association do not depend solely on a single molecular property, and we have previously shown that the use of an exhaustive, high throughput parameter search allows the rapid identification of predictive models.[28] To enable the elucidation of further association constant predictive models using

Table 3 List of parameters (*P*) used to produce association constant predictive models and computational method used to derive each parameter. A definition for each of these parameters can be found within the ESI (Table S46†)

			Derivation method	
P	*P* description	SI unit	PM6	B3LYP/6-31G*
P_1	E_{min}	kJ mol^{-1}		×
P_2	E_{max}	kJ mol^{-1}		×
P_3	Molecular volume	$Å^3$	×	
P_4	Molecular area	$Å^2$	×	
P_5	Solvent accessible area	$Å^2$	×	
P_6	Polar surface area	$Å^2$	×	
P_7	% Polar surface area	%	×	
P_8	Polarizability	C m^{-2}	×	
P_9	Steric weighting factor (SWF)	$Å^2$	×	
P_{10}	Steric accessibility factor (SAF)	$Å^2$	×	
P_{11}	HOMO	eV		×
P_{12}	LUMO	eV		×
P_{13}	Total energy	kJ		×
P_{14}	Electrostatic charge	C		×
P_{15}	Additive N···O bond length	Å		×
P_{16}	log *P*	N/A	×	
P_{17}	Dipole moment	D		×
P_{18}	Additive NH···O bond length	Å		×
P_{19}	H-Bond angle difference from optimal 180°	°		×

N/A = non-applicable. '×' identifies the computational modeling method used to generate the values for a particular parameter (*P*).

more than one computational parameter (Table 3), R data analysis software[52] was used to complete an exhaustive search of all potential parameter combinations for direct and inverse correlations of up to three parameters (eqn (1) and (2)). These searches included all relevant association constant data (Table 2) where $K_{ass} > 10$, to identify a single linear correlation.

$$K_{ass} = P_x^a \times P_y^b \quad |a| + |b| = 2 \tag{1}$$

$$K_{ass} = P_x^a \times P_y^b \times P_z^c \quad |a| + |b| + |c| = 3 \tag{2}$$

The form of these equations is suggested by the manner in which factors contribute to the free energy of binding and thus association constant.† The top 10 fits of these data to each of these two equations as identified through R^2 analysis are detailed within the supplementary materials. Although this approach did not result in the identification of any viable predictive models in this instance, it does offer an insight into which factors contribute to binding. Examination of the top 10 fits identified through either two parameter or three parameter searches shows that only some parameters exhibit any energetic significance, these results are summarised in Table 3. From this analysis, P_{10} (steric accessibility factor) and P_{14} (HBA electrostatic charge) are the two parameters that appear most commonly, with a total of 17 and 9 occurrences respectively; P_{11} (HOMO energy) is the third most common parameter, with 8 occurrences. The prevalence of P_{14} is not surprising as the electrostatic charge at the acceptor atoms would be expected to contribute to the electrostatic component of hydrogen bonding. Likewise, the HOMO energies, as associated with lone pairs at oxygen, will be involved in the potential for covalent contribution to the hydrogen bonding. More perplexing is the dominance of P_{10}, which describes the exposed electrophilic site of the simulant and not the HBA oxygen at all. However, the trends identified show an inverse correlation with P_{10} – the larger the exposed electrophilic site, the smaller the binding constant. This therefore corresponds to the steric bulk about the P or S atom and the extent to which the substituents are folded away from the electrophilic site and towards the HBA oxygens. We can therefore regard P_{10} as a proxy for steric bulk about the HBA centres. Taken together, these indicate that simple electrostatic models of hydrogen bonding are not sufficient to describe these systems, and that consideration of secondary bonding (and repulsive) interactions will be key in properly mimicking OP CWAs in future work (Table 4).

Table 4 Number of times a single parameter appears within the top 10 models, as identified through comparative R^2 analysis, obtained from an exhaustive search of P_1–P_{19} with eqn (1) and (2)

P	eqn (1)	eqn (2)	Total
P_1	1	2	3
P_2	0	0	0
P_3	0	0	0
P_4	0	0	0
P_5	0	0	0
P_6	0	1	1
P_7	0	0	0
P_8	0	0	0
P_9	0	0	0
P_{10}	8	9	17
P_{11}	4	4	8
P_{12}	0	0	0
P_{13}	0	0	0
P_{14}	4	5	9
P_{15}	2	2	4
P_{16}	0	0	0
P_{17}	0	3	3
P_{18}	1	4	5
P_{19}	0	0	0

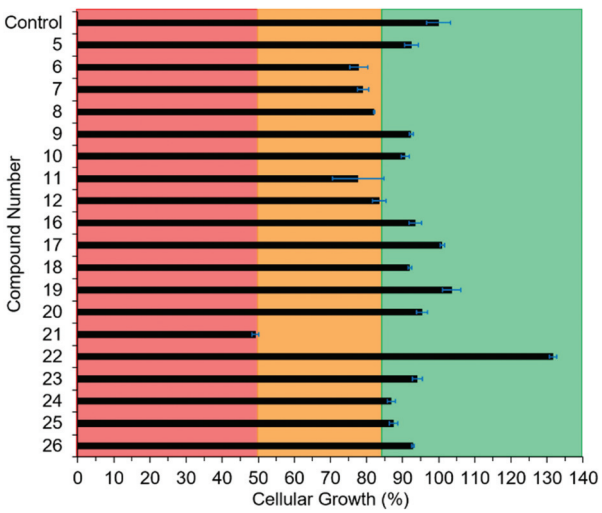

Fig. 5 *S. pombe* toxicity screening % cellular growth (recorded as maximum OD_{600}) reached at stationary phase in the presence of **5–12**, **16–26** (3.3 mM) relative to controls after 45 hours, supplied to the microbial broth solution in a 5% ethanol solution. Data shown represents an average of three experiments. Green – cell growth impeded by <16% over the course of 45 hours; Amber – cell growth impeded by 16–50% over the course of 45 hours; Red – cell growth impeded by >50% over the course of 45 hours. Control = 5% aqueous ethanol solution. Error = standard error of the mean.

Potential simulant toxicity

It is imperative that any simulants do not duplicate the toxicity of OP CWAs. The toxicity of these potential simulants against the commonly used model species *Schizosaccharomyces pombe (S. pombe)* was ascertained to gain some insight as to the potential toxicity of **5–12** and **16–26** towards eukaryotic cells in a biological environment.[53,54] The growth of this model yeast system was monitored by optical density measurements at 600 nm (OD_{600}) in the presence and absence of **5–12** and **16–26**, which were supplied in a 1 : 19 EtOH : H_2O solution to aid simulant solubility. The results of these studies are summarised in Fig. 5.

These preliminary results show that, at 3.3 mM, the simulants **5**, **8**, **10**, **16–20**, **22**, **25** and **26** have no significant impact

on cell growth therefore demonstrating little/no toxic effects, while simulants **6**, **7**, **9**, **11**, **12**, **21**, **23** and **24** show a degree of toxicity that warrants further investigation. The lead simulants identified to mimic complex formation for soman and sarin were shown to reduce the growth of *S. pombe* by 22.1%, 17.8%, 7.6%, 9.3%, 22.3% and 6.5% for **6**, **8–11**, and **16** respectively over a period of 45 h relative to control samples. This indicates simulants **8**, **10** and **16** pose no significant toxicity risk to eukaryotic organisms, while simulants **6**, **9** and **11** would require further investigation. It is also important to note that **17**, **19** and **22** showed greater than 100% cell growth and further investigations into this are underway. Nevertheless, full pharmacodynamic and pharmacokinetic studies should be undertaken before these simulants are considered safe to handle without the use of personal protective equipment.

Conclusions

We have produced a first-generation predictive model to aid in OP CWA simulant selection for the development of defensive technologies relating to OP CWA sensing through complexation, combining low level computational modelling and exhaustive parameter searches. The lead simulants currently identified using this model are **6** and **16** (for sarin), and **10** and **11** (for soman). Additionally, we hypothesise that the single parameter relationships identified here maybe developed towards the identification of solution state binding mode.

Finally, these results show that when choosing a simulant for the development of novel OP CWA detection and remediation methodologies, the specific physicochemical properties of interest should be considered. It is hoped that the uncovering of structure activity relationships achieved using similar parametric searching methodologies to those detailed herein will enable the evermore effective identification of appropriate simulants to aid in the development of novel technologies for the effective detection of OP CWAs. Our work in this area is ongoing as we seek to apply this highly accessible methodology to enable the identification of suitable simulants not only for CWAs but also for pesticides, a common agricultural pollutant.

Conflicts of interest

There are no conflicts to declare.

Acknowledgements

J. Hiscock and R. Ellaby would like to thank the University of Kent for funding. We would also like to thank K. Howland (School of Biosciences, University of Kent) for his mass spectrometry assistance.

Notes and references

1 R. T. Delfino, T. S. Ribeiro and J. D. Figueroa-Villar, *J. Braz. Chem. Soc.*, 2009, **20**, 407–428.
2 German Federal Government, Statement by the Federal Government on the Navalny case, https://www.bundesregierung.de/breg-en/news/statement-by-the-federal-government-on-thenavalny-case-1781882 (accessed 24th September 2020).
3 M. Peplow, *Chem. Eng. News*, 2018, **96**, 3–3.
4 T. Nakagawa and A. T. Tu, *Forensic Toxicol.*, 2018, **36**, 542–544.
5 H. John, M. J. van der Schans, M. Koller, H. E. T. Spruit, F. Worek, H. Thiermann and D. Noort, *Forensic Toxicol.*, 2018, **36**, 61–71.
6 T. Okumura, N. Takasu, S. Ishimatsu, S. Miyanoki, A. Mitsuhashi, K. Kumada, K. Tanaka and S. Hinohara, *Ann. Emerg. Med.*, 1996, **28**, 129–135.
7 M. R. Sambrook and S. Notman, *Chem. Soc. Rev.*, 2013, **42**, 9251–9267.
8 B. D. de Grenu, D. Moreno, T. Torroba, A. Berg, J. Gunnars, T. Nilsson, R. Nyman, M. Persson, J. Pettersson, I. Eklind and P. Wasterby, *J. Am. Chem. Soc.*, 2014, **136**, 4125–4128.
9 G. H. Dennison, C. G. Bochet, C. Curty, J. Ducry, D. J. Nielsen, M. R. Sambrook, A. Zaugg and M. R. Johnston, *Eur. J. Inorg. Chem.*, 2016, **9**, 1348–1358.
10 G. H. Dennison, M. R. Sambrook and M. R. Johnston, *RSC Adv.*, 2014, **4**, 55524–55528.
11 G. H. Dennison, M. R. Sambrook and M. R. Johnston, *Chem. Commun.*, 2014, **50**, 195–197.
12 M. R. Sambrook, J. R. Hiscock, A. Cook, A. C. Green, I. Holden, J. C. Vincent and P. A. Gale, *Chem. Commun.*, 2012, **48**, 5605–5607.
13 J. R. Hiscock, N. J. Wells, J. A. Ede, P. A. Gale and M. R. Sambrook, *Org. Biomol. Chem.*, 2016, **14**, 9560–9567.
14 J. R. Hiscock, M. R. Sambrook, P. B. Cranwell, P. Watts, J. C. Vincent, D. J. Xuereb, N. J. Wells, R. Raja and P. A. Gale, *Chem. Commun.*, 2014, **50**, 6217–6220.
15 J. R. Hiscock, I. L. Kirby, J. Herniman, G. J. Langley, A. J. Clark and P. A. Gale, *RSC Adv.*, 2014, **4**, 45517–45521.
16 J. R. Hiscock, M. R. Sambrook, J. A. Ede, N. J. Wells and P. A. Gale, *J. Mater. Chem. A*, 2015, **3**, 1230–1234.
17 J. R. Hiscock, M. R. Sambrook, N. J. Wells and P. A. Gale, *Chem. Sci.*, 2015, **6**, 5680–5684.
18 H. Cave, J. A. Ede, M. R. Sambrook, H. Dodd, F. Fucassi, A. S. Cragg, A. H. Lansley and P. J. Cragg, *Supramol. Chem.*, 2019, **31**, 703–712.
19 C. G. P. Taylor, J. R. Piper and M. D. Ward, *Chem. Commun.*, 2016, **52**, 6225–6228.
20 C. G. P. Taylor, A. J. Metherell, S. P. Argent, F. M. Ashour, N. H. Williams and M. D. Ward, *Chem. – Eur. J.*, 2020, **26**, 3065–3073.
21 J. A. Ede, P. J. Cragg and M. R. Sambrook, *Molecules*, 2018, **23**(1), 207–219.
22 M. R. Sambrook, I. A. Gass and P. J. Cragg, *Supramol. Chem.*, 2018, **30**, 206–217.

23 M. R. Sambrook, J. C. Vincent, J. A. Ede, I. A. Gass and P. J. Cragg, *RSC Adv.*, 2017, **7**, 38069–38076.
24 S. L. Bartelt-Hunt, D. R. U. Knappe and M. A. Barlaz, *Crit. Rev. Environ. Sci. Technol.*, 2008, **38**, 112–136.
25 M. L. Medonca and R. Q. Snurr, *Chem. – Eur. J.*, 2019, **25**, 9217–9229.
26 L. J. White, S. N. Tyuleva, B. Wilson, H. J. Shepherd, K. K. L. Ng, S. J. Holder, E. R. Clark and J. R. Hiscock, *Chem. – Eur. J.*, 2018, **24**, 7761–7773.
27 L. J. White, N. J. Wells, L. R. Blackholly, H. J. Shepherd, B. Wilson, G. P. Bustone, T. J. Runacres and J. R. Hiscock, *Chem. Sci.*, 2017, **8**, 7620–7630.
28 N. Allen;, L. J. White, J. E. Boles, G. T. Williams, D. F. Chu, R. J. Ellaby, H. J. Shepherd, K. K. L. Ng, L. R. Blackholly, B. Wilson, D. P. Mulvihill and J. R. Hiscock, *ChemMedChem*, 2020, **15**, 2193–2205.
29 N. Busschaert, I. L. Kirby, S. Young, S. J. Coles, P. N. Horton, M. E. Light and P. A. Gale, *Angew. Chem., Int. Ed.*, 2012, **51**, 4426–4430.
30 C. M. Chau, T. J. Chuan and K. M. Liu, *RSC Adv.*, 2014, **4**, 1276–1282.
31 S. M. S. Chauhan, B. Garg and T. Bisht, *Molecules*, 2007, **12**, 2458–2466.
32 Y. F. Chen, C. L. Kao, W. K. Lee, P. C. Huang, C. Y. Hsu and C. H. Kuei, *J. Chin. Chem. Soc.*, 2016, **63**, 751–757.
33 D. S. Panmand, A. D. Tiwari, S. S. Panda, J. C. M. Monbaliu, L. K. Beagle, A. M. Asiri, C. V. Stevens, P. J. Steel, C. D. Hall and A. R. Katritzky, *Tetrahedron Lett.*, 2014, **55**, 5898–5901.
34 H. Huang, J. Ash and J. Y. Kang, *Org. Lett.*, 2018, **20**, 4938–4941.
35 S. M. Feng, J. Li and J. F. Wei, *New J. Chem.*, 2017, **41**, 4743–4746.
36 D. V. Schoonover and H. W. Gibson, *Tetrahedron Lett.*, 2017, **58**, 242–244.
37 J. W. W. Chang, E. Y. R. Chia, C. L. L. Chai and J. Seayad, *Org. Biomol. Chem.*, 2012, **10**, 2289–2299.
38 T. Noji, H. Fujiwara, K. Okano and H. Tokuyama, *Org. Lett.*, 2013, **15**, 1946–1949.
39 N. Ortega, A. Feher-Voelger, M. Brovetto, J. I. Padron, V. S. Martin and T. Martin, *Adv. Synth. Catal.*, 2011, **353**, 963–972.
40 J. J. Wang, Y. Y. Zhao, W. Zhao, P. Wang and J. Li, *J. Carbohydr. Chem.*, 2016, **35**, 445–454.
41 P. Thordarson, K. Sewell and V. Efremova, supramolecular.org.
42 F. Ulatowski, K. Dabrowa, T. Balakier and J. Jurczak, *J. Org. Chem.*, 2016, **81**, 1746–1756.
43 M. Walker, A. J. A. Harvey, A. Sen and C. E. H. Dessent, *J. Phys. Chem. A*, 2013, 12590–12600.
44 M. J. Frisch, G. W. Trucks, H. B. Schlegel, G. E. Scuseria, M. A. Robb, J. R. Cheeseman, G. Scalmani, V. Barone, G. A. Petersson, H. Nakatsuji, X. Li, M. Caricato, A. V. Marenich, J. Bloino, B. G. Janesko, R. Gomperts, B. Mennucci, H. P. Hratchian, J. V. Ortiz, A. F. Izmaylov, J. L. Sonnenberg, D. Williams-Young, F. Ding, F. Lipparini, F. Egidi, J. Goings, B. Peng, A. Petrone, T. Henderson, D. Ranasinghe, V. G. Zakrzewski, J. Gao, N. Rega, G. Zheng, W. Liang, M. Hada, M. Ehara, K. Toyota, R. Fukuda, J. Hasegawa, M. Ishida, T. Nakajima, Y. Honda, O. Kitao, H. Nakai, T. Vreven, K. Throssell, J. A. Montgomery Jr., J. E. Peralta, F. Ogliaro, M. J. Bearpark, J. J. Heyd, E. N. Brothers, K. N. Kudin, V. N. Staroverov, T. A. Keith, R. Kobayashi, J. Normand, K. Raghavachari, A. P. Rendell, J. C. Burant, S. S. Iyengar, J. Tomasi, M. Cossi, J. M. Millam, M. Klene, C. Adamo, R. Cammi, J. W. Ochterski, R. L. Martin, K. Morokuma, O. Farkas, J. B. Foresman and D. J. Fox, *Gaussian 16, Revision A.03*, Gaussian Inc., Wallingford CT, 2016.
45 A. D. McLean and G. S. Chandler, *J. Chem. Phys.*, 1980, **72**, 5639–5648.
46 A. F. Rodrigues-Oliveira, F. W. M. Ribeiro, G. Cervi and T. C. Correra, *ACS Omega*, 2018, **3**, 9075–9085.
47 Y. Shao, L. F. Molnar, Y. Jung, J. Kussmann, C. Ochsenfeld, S. T. Brown, A. T. B. Gilbert, L. V. Slipchenko, S. V. Levchenko, D. P. O'Neill, R. A. DiStasio Jr., R. C. Lochan, T. Wang, G. J. O. Beran, N. A. Besley, J. M. Herbert, C. Y. Lin, T. Van Voorhis, S. H. Chien, A. Sodt, R. P. Steele, V. A. Rassolov, P. E. Maslen, P. P. Korambath, R. D. Adamson, B. Austin, J. Baker, E. F. C. Byrd, H. Dachsel, R. J. Doerksen, A. Dreuw, B. D. Dunietz, A. D. Dutoi, T. R. Furlani, S. R. Gwaltney, A. Heyden, S. Hirata, C.-P. Hsu, G. Kedziora, R. Z. Khalliulin, P. Klunzinger, A. M. Lee, M. S. Lee, W. Z. Liang, I. Lotan, N. Nair, B. Peters, E. I. Proynov, P. A. Pieniazek, Y. M. Rhee, J. Ritchie, E. Rosta, C. D. Sherrill, A. C. Simmonett, J. E. Subotnik, H. L. Woodcock III, W. Zhang, A. T. Bell, A. K. Chakraborty, D. M. Chipman, F. J. Keil, A. Warshel, W. J. Hehre, H. F. Schaefer, J. Kong, A. I. Krylov, P. M. W. Gill and M. Head-Gordon, *Phys. Chem. Chem. Phys.*, 2006, **8**, 3172–3191.
48 C. A. Hunter, *Angew. Chem., Int. Ed.*, 2004, **43**, 5310–5324.
49 J. J. P. Stewart, *J. Mol. Model.*, 2007, **13**, 1173–1213.
50 L. R. Blackholly, H. J. Shepherd and J. R. Hiscock, *CrystEngComm*, 2016, **18**, 7021–7028.
51 T. Steiner, *Angew. Chem., Int. Ed.*, 2002, **41**, 48–76.
52 R Core Team, *R: A language and environment for statistical computing*, R Foundation for Statistical Computing, Vienna, Austria, 2018, https://www.R-project.org/.
53 J. Hayles and P. Nurse, *Introduction to Fission Yeast as a Model System*, Cold Sping Harbor Protocols, 2018.
54 X. H. Gan, J. Yang, J. Li, H. Y. Yu, H. M. Dai, J. Y. Liu and Y. Huang, *Biochem. J.*, 2011, **435**, 103–111.
55 G. M. Sheldrick, *Acta Crystallogr., Sect. A: Found. Adv.*, 2015, **71**, 3–8.
56 G. M. Sheldrick, *Acta Crystallogr., Sect. C: Struct. Chem.*, 2015, **71**, 3–8.
57 O. V. Dolomanov, L. J. Bourhis, R. J. Gildea, J. A. K. Howard and H. Puschmann, *J. Appl. Crystallogr.*, 2009, **42**, 339–341.